17th World Conference on Earthquake Engineering, 17WCEE
Sendai, Japan - September 13th to 18th 2020

MULTIPLE SUPPORT EXCITATION PROBLEM FOR UNDERGROUND STRUCTURE

N. Yoshida[(1)], S. Sawada[(2)], H. Goto[(3)]

[(1)] *Professor, Kanto Gakuin University, boh070949@gmail.com*
[(2)] *Professor, Kyoto University, sawada@catfish.dpri.kyoto-u.ac.jp*
[(3)] *Associate Professor, Kyoto University, goto@catfish.dpri.kyoto-u.ac.jp*

Abstract

Formulation for the multiple support excitation problem for the seismic response analysis of underground structures is presented and discussed. A soil-structure interaction model is separated into a structure including underground structures and a ground. Response of the ground is calculated at first. Then output of the ground is applied to the structural part as multi excitation problem. This method requires velocity and displacement time history at the interface between soil and structure in addition to the input earthquake motion. Applicability of the proposed method is examined by two case studies. One is a pile foundation in a liquefied ground and the other is a water pipeline under obliquely incident wave. Horizontal pipeline and pipeline with T shape connections are analyzed in the latter case. In both study, the case that soil-structural problem solved in one analysis and the case by using multiple support excitation analysis in which a ground and a structure is solved separately give identical solutions. In addition, the first case study shows both displacement and velocity input is necessary. It is also shown that inertia force of the pile is not important and is negligible. In the second case study, both inertial force and velocity input is shown not to be important; underground water pile can be solved under displacement input only. Difference between two case studies comes from the viscous coefficient of the interaction spring connecting the pipeline and the ground. The Rayleigh damping, which is frequently used damping in the seismic response analysis, automatically specify velocity dependent property that is too large for the interaction spring. Finally, as more realistic problem, an underground pipeline that has T-shape connection is analyzed. Bending moment at the joint is largest, which implies that damage to pipeline frequently occurs at the joint. It is shown that the ultimate strength of the interaction spring is also an important factor.

Keywords: earthquake, multiple support excitation, underground structure, seismic deformation method, obliquely incident wave

1. Introduction

There are several cases that multiple support excitation are required in the seismic response analysis.

One is the case that different earthquake motions input in a structure, which is schematically shown in Fig. 1 where input earthquake motions at both foundations are different to each other. Long bridge is one of the typical examples in this case. Formulation of this case was already proposed by Clough and Penzien [1]

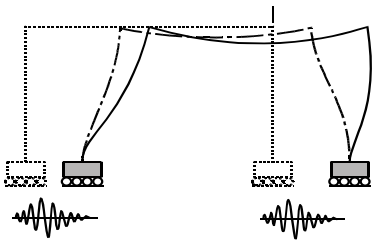

Fig. 1 – Schematic model showing different input motion at two foundations

Another example is a soil-structure interaction problem such as Fig. 2(a). This model was originally proposed by Penzien [2], and has been widely used by improving or extending [3, 4]. Fig. 2(b) is an example of extended Penzien model [4]. However, using this kind of model includes some difficulties. Both soil and structure will behave in nonlinear manners under very large earthquakes. Constitutive models for severely nonlinear behavior has become complicated to consider strong nonlinearity. Generally speaking, a computer program designed for soil does not have complicated nonlinear model for structural members and vice versa. Therefore, it is not realistic to solve a soil-structure system as one model. Multiple support excitation can be used in these cases; the model in Fig. 2(a) is separately modeled as shown in Fig. 2(c). Then the ground and the structure can be solved separately; the only requirement to the computer program is to add displacement and velocity input in the conventional seismic response analysis procedure as shown in the next chapter. Formulation of this case was proposed by the authors [5]. The spring connecting the structure and the ground is called several names such as (dynamic) Winkler spring, soil-structure interaction spring and ground spring, etc. It is called interaction spring in this paper for simplicity.

This paper will present detailed investigation of the formulation and several case studies to obtain notes in using the multi excitation problem in the engineering practice.

2. Formulation of multiple support excitation

2.1 Fundamentals

Equation of motion for a multiple degrees of freedom is expressed as

$$\mathbf{M}\ddot{\mathbf{u}}^t + \mathbf{C}\dot{\mathbf{u}}^t + \mathbf{K}\mathbf{u}^t = \mathbf{0} \tag{1}$$

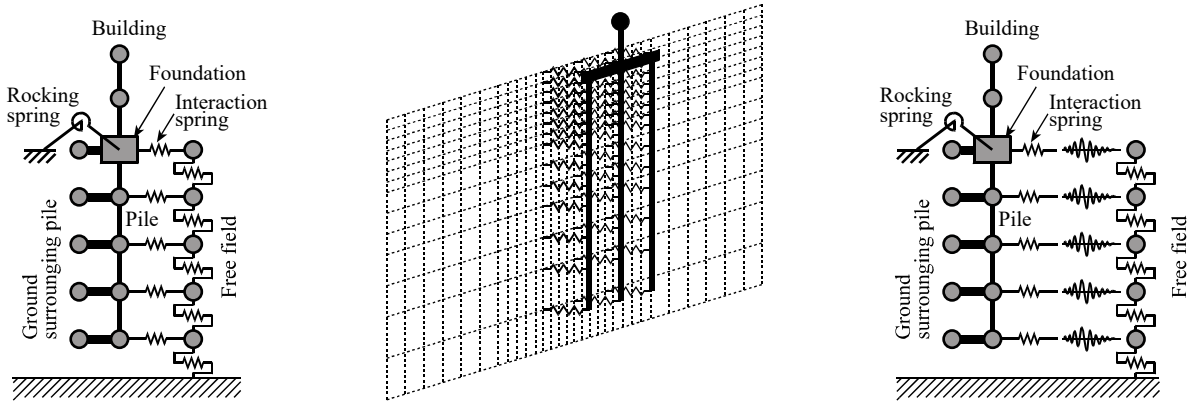

(a) Penzien model (b) 2D model (c) Multile excitation model

Fig. 2 – Soil-structure interaction problem

where **M**, **C**, and **K** denote mass, damping, and stiffness matrix, respectively, and $\mathbf{u}^t$ denotes absolute displacement. Bold character indicates matrix or vector and dot denotes derivative with respect to time. Absolute displacement $\mathbf{u}^t$ is separated into rigid displacement (displacement at which earthquake motion incident or reference point) $\mathbf{u}^R$ and displacement relative to reference point **u**, as

$$\mathbf{u}^t = \begin{Bmatrix} \mathbf{u}_a^t \\ \mathbf{u}_b^t \end{Bmatrix} = \begin{Bmatrix} \mathbf{u}_a^R \\ \mathbf{u}_b^R \end{Bmatrix} + \begin{Bmatrix} \mathbf{u}_a \\ \mathbf{u}_b \end{Bmatrix} \tag{2}$$

where subscript *a* and *b* denote free component and excited component, respectively. Then Eq. (1) is rewritten as

$$\begin{bmatrix} \mathbf{M}_a & \mathbf{0} \\ \mathbf{0} & \mathbf{M}_b \end{bmatrix} \begin{Bmatrix} \ddot{\mathbf{u}}_a^R + \ddot{\mathbf{u}}_a \\ \ddot{\mathbf{u}}_b^R + \ddot{\mathbf{u}}_b \end{Bmatrix} + \begin{bmatrix} \mathbf{C}_{aa} & \mathbf{C}_{ab} \\ \mathbf{C}_{ba} & \mathbf{C}_{bb} \end{bmatrix} \begin{Bmatrix} \dot{\mathbf{u}}_a^R + \dot{\mathbf{u}}_a \\ \dot{\mathbf{u}}_b^R + \dot{\mathbf{u}}_b \end{Bmatrix} + \begin{bmatrix} \mathbf{K}_{aa} & \mathbf{K}_{ab} \\ \mathbf{K}_{ba} & \mathbf{K}_{bb} \end{bmatrix} \begin{Bmatrix} \mathbf{u}_a^R + \mathbf{u}_a \\ \mathbf{u}_b^R + \mathbf{u}_b \end{Bmatrix} = \begin{Bmatrix} \mathbf{0} \\ \mathbf{0} \end{Bmatrix} \tag{3}$$

Here, lumped mass is assumed, but formulation for consistent mass is easily done using the same procedure below. Taking the free degree of freedom component (the first equation), we obtains

$$\mathbf{M}_a \ddot{\mathbf{u}}_a + \mathbf{C}_{aa} \dot{\mathbf{u}}_a + \mathbf{K}_{aa} \mathbf{u}_a = -\mathbf{M}_a \mathbf{I}_a \ddot{\mathbf{u}}_a^R - \mathbf{C}_{ab} \dot{\mathbf{u}}_b - \mathbf{K}_{ab} \mathbf{u}_b \tag{4}$$

where component of $\mathbf{I}_a$ takes 1 when there is degree of freedom in the direction of earthquake motion, and 0 for other case; it is an expression of Kronecker's delta in matrix expression. Here, $\mathbf{K}_{aa}\mathbf{u}_a^R$ and $\mathbf{K}_{aa}\dot{\mathbf{u}}_a^R$ are deleted because resulting vector is null. Moreover, damping term proportional to relative velocity is also deleted because it is deleted in the ordinary equation of motion.

This equation is exactly same equation with ordinary equation of motion except there is two term in the right hand, $\mathbf{C}_{ab}\dot{\mathbf{u}}_b$ and $\mathbf{K}_{ab}\mathbf{u}_b$. This means that both displacement and velocity are necessary at the excited degree of freedom.

2.2 Difference from conventional analysis

In the conventional analysis, which solves soil-structure system in one time and is called whole analysis hereafter, equation of motion is expressed by the incremental form as

$$\mathbf{M}d\ddot{\mathbf{u}} + \mathbf{C}d\dot{\mathbf{u}} + \mathbf{K}d\mathbf{u} = -\mathbf{M}\mathbf{I}d\ddot{\mathbf{u}}^R \tag{5}$$

Let's consider to solve this equation by the Newmark's β method, for example, resulting simultaneous equation to obtain displacement incremrnt d**u** yields

$$\left(\frac{\mathbf{M}}{\beta dt^2} + \frac{\gamma \mathbf{C}}{\beta dt} + \mathbf{K}\right) d\mathbf{u} = \mathbf{M}\left(\frac{\dot{\mathbf{u}}_{t-dt}}{\beta dt} + \frac{\ddot{\mathbf{u}}_{t-dt}}{2\beta}\right) + \mathbf{C}\left(\frac{\gamma \dot{\mathbf{u}}_{t-dt}}{\beta} - \left(1 - \frac{\gamma}{2\beta}\right) dt \ddot{\mathbf{u}}_{t-dt}\right) - \mathbf{M}_a \mathbf{I} d\ddot{\mathbf{u}}^R \tag{6}$$

Here γ=0.5 is frequently used. This equation includes both structure and soil freedoms, and they are separated by using subscript *a* and *b* same as above. Then, we obtain

$$\begin{aligned} \left(\frac{\mathbf{M}_a}{\beta dt^2} + \frac{\gamma \mathbf{C}_{aa}}{\beta dt} + \mathbf{K}_{aa}\right) d\mathbf{u}_a = &-\frac{\mathbf{C}_{ab}\dot{\mathbf{u}}_b}{\beta dt} - \mathbf{K}_{ab} d\mathbf{u}_b + \mathbf{M}_a \left(\frac{\dot{\mathbf{u}}_a}{\beta dt} + \frac{\ddot{\mathbf{u}}_a}{2\beta}\right) + \mathbf{C}_{aa}\left(\frac{\gamma \dot{\mathbf{u}}_a}{\beta} - \left(1 - \frac{\gamma}{2\beta}\right) dt \ddot{\mathbf{u}}_a\right) \\ &+ \mathbf{C}_{ab}\left(\frac{\gamma \dot{\mathbf{u}}_b}{\beta} - \left(1 - \frac{\gamma}{2\beta}\right) dt \ddot{\mathbf{u}}_b\right) - \mathbf{M}\mathbf{I} d\ddot{\mathbf{u}}^R \end{aligned} \tag{7}$$

Here, $\mathbf{u}_{t\text{-}dt}$ is written just as **u**.

In the same manner, by applying the Newmark's β method, Eq. (4) yields

$$\left(\frac{\mathbf{M}_a}{\beta dt^2}+\frac{\gamma\mathbf{C}_{aa}}{\beta dt}+\mathbf{K}_{aa}\right)d\mathbf{u}_a = \\ -\mathbf{C}_{ab}d\dot{\mathbf{u}}_b-\mathbf{K}_{ab}d\mathbf{u}_b+\mathbf{M}_a\left(\frac{\dot{\mathbf{u}}_a}{\beta dt}+\frac{\ddot{\mathbf{u}}_a}{2\beta}\right)+\mathbf{C}_{aa}\left(\frac{\gamma\dot{\mathbf{u}}_a}{\beta}-\left(1-\frac{\gamma}{2\beta}\right)dt\ddot{\mathbf{u}}_a\right)-\mathbf{M}\mathbf{I}d\ddot{\mathbf{u}}^R \tag{8}$$

There are some differences in the right hand side of Eqs. (7) and (8). They are

Whole analysis: $\mathbf{C}_{ab}\left(\frac{\gamma\dot{\mathbf{u}}_b}{\beta}-\left(1-\frac{\gamma}{2\beta}\right)dt\ddot{\mathbf{u}}_b\right)$

Multiple support excitation: $-\mathbf{C}_{ab}d\dot{\mathbf{u}}_b$

This difference comes from the assumption in the numerical integration. In the whole analysis, response of each degree of freedom is evaluated by an interpolation function that integral scheme is assumed. On the other hand, in the multiple support excitation formulation, response at the excited degree of freedom is given as a response of the ground part. Therefore, if the same integral scheme is used for both analysis, i.e., the ground and the multiple support excitation analyses, right hand sides become same; same solution is obtained.

3. Pile foundation

A building whose pile foundation was damaged during the 1995 Kobe earthquake [4] is analyzed. However, degree of damage is out of interest in this paper because of two reasons. The one is that damage to the pile is caused mainly by the liquefaction-induced flow that is not considered in this study. The site is located in the Fukaehama reclaimed land, Kobe city, and is located about 350 m from the seawall (Point A in Fig. 3). In the same island, there was a pile foundation for a building located about 400 m from the seawall (Point B in Fig. 3), but building was not constructed. Detailed investigation of the pile showed that direction of damaged pile is toward the seawall, but not toward the predominant direction of ground shaking [6]. It indicates damage of the pile is caused by the liquefaction-induced flow. Direction of displacement near the site of the analyed pile is also perpendicular to the predominant direction of earthquake shaking. Therefore, comparison with the damage does not have practical meaning. The second is that, as described in chapter 1, applicability of multiple support erexcitation formulation is interested in this paper.

Fig. 4 shows acceleration time history observed at Higashi Kobe Bridge that is located at point C in Fig. 3. FEM model is shown in Fig. 5(a). The pile is modeled as a beam and is connected to the ground by interaction springs. The ground is modeled as one-dimensional ground. Here, if this model is analyzed as it is, behavior of the pile affects the behavior of ground, which is not a good model. One solution to solve this problem approximately is to use large mass for the ground so that effect of pile becomes negligible. In order to avoid the effect of pile to the ground perfectly, however, a spring element to work in one directional only is employed in this calculation. The force-displacement relationships are expressed as

$$\begin{Bmatrix} F_g \\ F_s \end{Bmatrix} = \begin{bmatrix} 0 & 0 \\ -K & K \end{bmatrix} \begin{Bmatrix} u_g \\ u_s \end{Bmatrix} \tag{9}$$

where K is a spring constant and F and u are force and diaplacement, respectively. Subscripts s and g denote structural and ground sides, respectively. The stiffness matrix becomes asymmetric by using this matrix, but it is not a problem in the analysis of ground because stiffness matrix is asymmetric when non-associated flow rule is used for soil.

Unit weight γ and shear wave velocity V_s of soil is shown in Fig. 5 (a), and cyclic shear deformation characteristics is shown in Fig. 6. Shear stress-shear strain model used in this analysis can simulate cyclic shear deformation characteristics perfectly [7].

Coefficient of subgrade reaction k_H of the ground is evaluated based on the Specification for Highway Bridge [8], as

$$k_H = k_{h0}(B_H / 0.3)^{-3/4} \tag{10}$$

where B_H denotes width of the pile in meter and

$$k_{H0} = \alpha E_0 / 0.3 \tag{11}$$

Here, E_0 denotes Young's modulus and is evaluated from SPT-N value as

$$E_0 = 2800N \ \ (\mathrm{kN/m^2}) \tag{12}$$

and α is a coefficient depending on the method to evaluate Young's modulus and is 2 in this case. Ultimate subgrade reaction p_y is evaluated based on Kishida and Nakai [9], which is expressed as

$$\begin{aligned} &\text{Sand: } p_y = 3\tan^2(45+\phi/2)\gamma_t' z \\ &\text{Clay: } p_y = 9c_u \end{aligned} \tag{13}$$

Here, internal friction angle ϕ and cohesion c_u are set 30 degree and 10 kPa. However, considering the fact that liquefaction occurred in this site, spring constant of the interaction spring is reduced to 1/10 of the original model for sand layers under the water table.

The pile is modeled as a nonlinear beam element, which is shown in Fig. 7, where yield bending moment M_y and ultimate moment M_u are 129.08 kNm and 183.43 kNm, respectively, and the second and third gradients are 9.54 and 0.7 % of the initial modulus, respectively.

Damping matrix $\mathbf{C}$ is calculated by Rayleigh damping, as

$$\mathbf{C} = \alpha\mathbf{M} + \beta\mathbf{K} \ \ (\mathrm{kN/m^2}) \tag{14}$$

where coefficient are set α=0 and β=0.005.

Result of the whole analysis is summarized in Fig. 5(b), in which the ground is expressed as one line.

Three calculations are conducted in addition to the whole analysis, which are

① Consider all load in Eq. (4). Displacement and velocity are applied in addition to the inertia term.
② Among three component above, velocity is not applied.
③ Among three component above, inertia term is not applied.

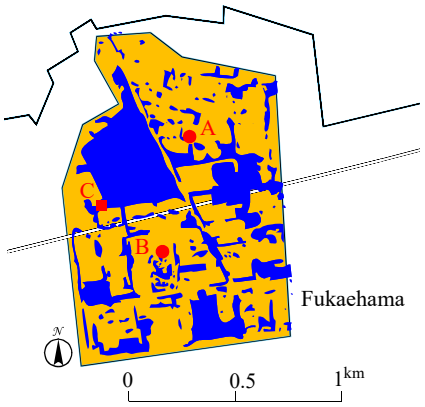

Fig. 3 – Map showing locations and sand boil (ocher color)

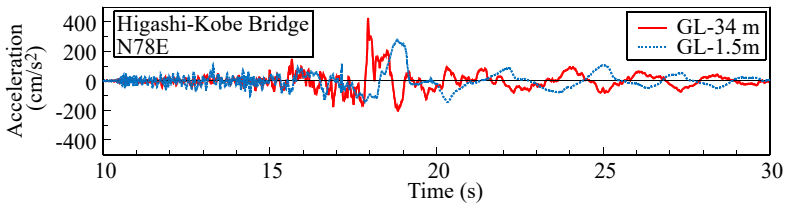

Fig. 4 – Acceleration observed at Higashi-Kobe Bridge

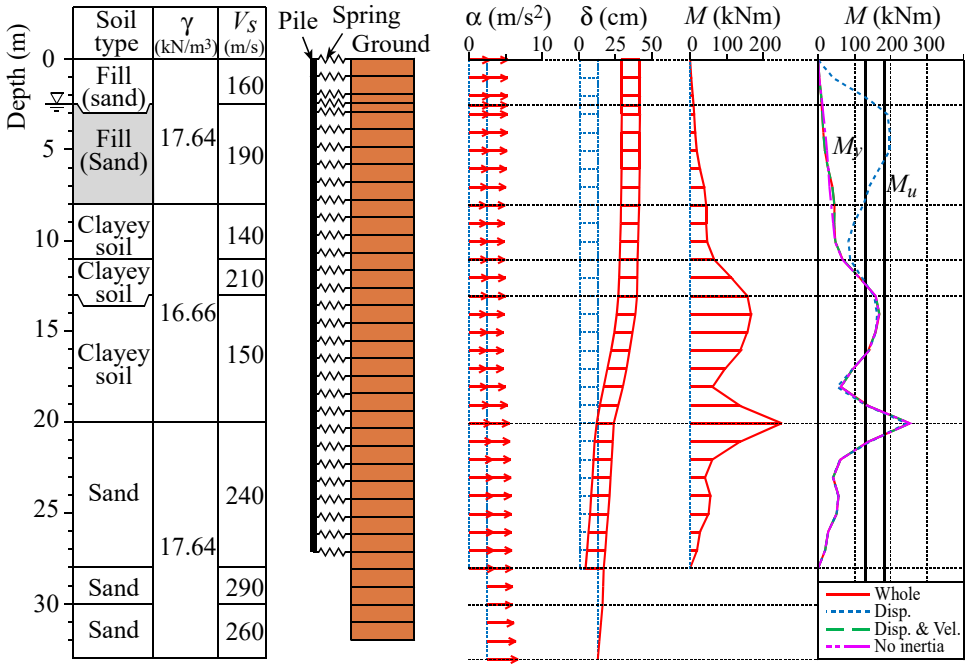

(a) Model (b) Whole analysis (b) Multiple support excitation

Fig. 5 –Pile model and maximum responses

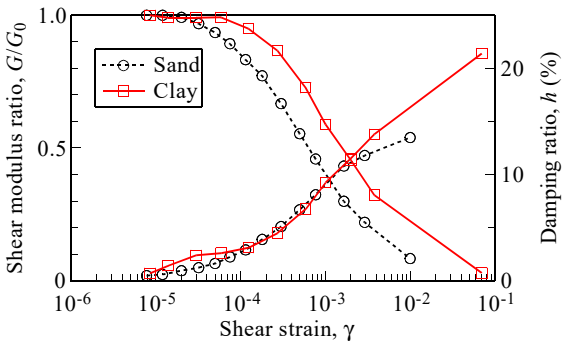

Fig. 6 – Cyclic shear deformation characteristics

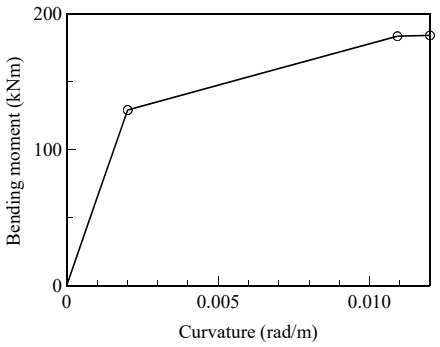

Fig. 7 – Moment-curvature relationships

Result of the analyses is summrized in Fig. 5(c). The whole analysis (whole in Fig. 5(c)) and ① the case to consider all terms (Disp. & Vel. in Fig. 5(c)) are identical. There is very small difference between the whole analysis and ③ (No inertia in Fig. 5(c). There are, hoever, significant differences between the whole analysis and ② (Disp. in Fig. 5(c)).

In the engineering practice to analyze a pile during earthquake, seismic deformation method is frequently used. In this method, deformation of the ground is applied through the interaction spring statically. Compared with the multiple support excitation analysis, there are two key points, except that seismic deformation analysis uses displacement of the ground at a particular time or a maximum displacement whereas multiple support excitation analysis conducts time marching analysis. The one is that inertial force of the pile is not considered although inertial force from superstructure is frequently considered. The second is that velocity is not considered. Looking at the result shown in Fig. 5(c), neglecting inertia force of the pile is justified, but velocity term is important.

4. Underground lineal structure under obliquely propagating wave

Ground deformation is supposed to be one of the important factor in the seismic design of an underground lineal structure such as water and gas pipelines. However, no stress occurs in the underground structure in the horizontally layered ground under the vertically propagating earthquake motion, because ground displacement is same at same depths. Therefore, affecting ground deformation is caused by a surface wave or obliquely propagating body wave. Obliquely propagating S wave is considered in this paper.

Fig. 8 shows FEM model with soil properties. A large mass method is used in this analysis, in which the width of the model is 100 m. The S wave propagates 15 degree from the vertical axis. Lateral boundary is set parallel to the direction of wave propagation and allowed to move only perpendicular direction to the lateral boundary. Earthquake motion is defined as incident wave; an engineering seismic base layer with V_s=500 m/s is assumed. Since maximum mesh size in the direction of wave propagation is 6 m, frequencies smaller than 5 to 6Hz is interested. A polyethylene water supply pipeline with 93 mm external diameter are put at GL-6 m. This depth is deeper than the depth for ordinary water supply pipelines. It comes from the mesh size, but it does not affect the discussion in this paper. Young's modulus of the pipeline is 1100 MN/m^2. Coefficient of subgrade reaction of the ground is evaluated based on the Earthquake-proof Method Criteria for Waterworks [10], which is same with Ref. [8].

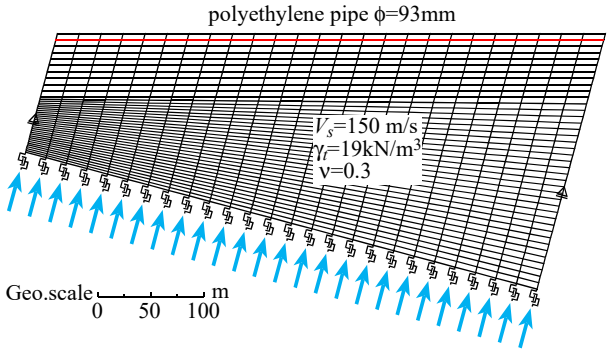

Fig. 8 – FEM model

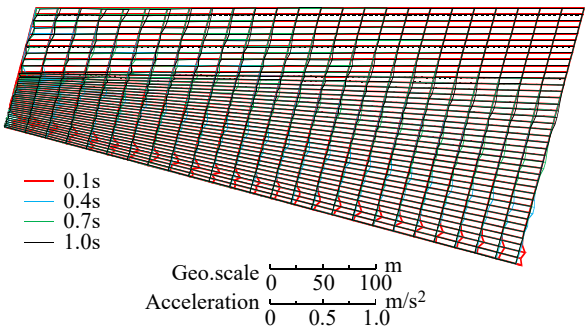

Fig. 9 – Wave propagation under pulse wave

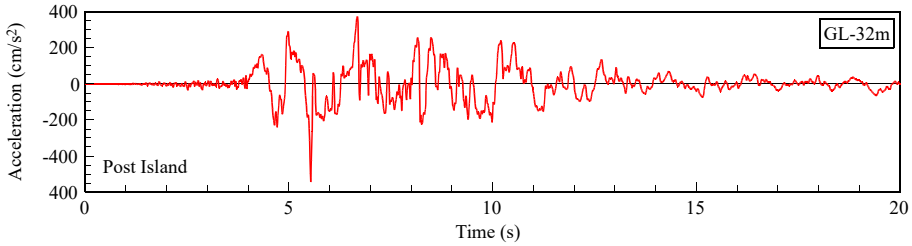

Fig. 10 – Acceleration observed at GL-32 m in Port Island

Fig. 9 shows acceleration distribution at several times under pulse wave input in order to confirm that the wave propagate correctly, and is well expressed. Then, earthquake motion observed during the 1995 Kobe earthquake at Port Island (GL-32m, NS component, Fig. 10) is used as incident wave. Since it is supposed that reflected wave at the boundary may affect the response, earthquake motion is cut from 4 to 7 s is used.

This analysis is focused on velocity proportional nature of the interaction spring. As shown in Eq. (4),

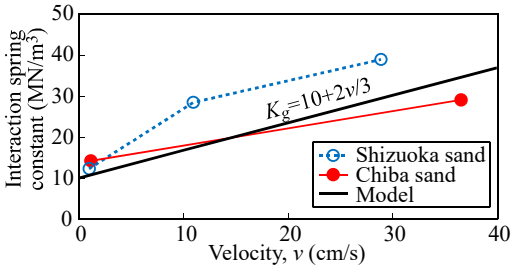

Fig. 11 – Velocity dependent spring constant

velocity need not be considered if $\mathbf{C}_{ab}$ is very small. Result in chapter 3 indicates that Rayleigh damping with β=0.005 is not small value. Therefore, it is reduced to β=0.0005. Shimamura et al. [11], for example, showed velocity proportional characteristics based on real scale test as shown in Fig. 11. Two different soil, Shizuoka sand and Chiba sand, show somewhat different characteristics. For the simplicity of the analysis, a solid line in the figure is used, where v denotes velocity. Then, interaction spring has static rigidity and velocity proportional rigidity. Here, it is noted that model in Fig. 11 is the result of steel pile with 600 mm external diameter. It is modified for the pipeline in this analysis (93 mm external diameter), which is already shown in chapter 3. The velocity proportional term can be modeled by a stiffness proportional damping with coefficient 6.82.

Five cases, ①~⑤ are conducted, where
① whole analysis
② multiple support excitation analysis considers all terms
③ multiple support excitation analysis, but velocity is not used
④ static analysis to apply ground displacement obtained by ①
⑤ same as ① and velocity dependency of the interaction spring

Maximum bending moment of the analysis is shown in Fig. 12. Here, cases ① and ② are exactly same; therefore, only one result is shown as solid black line. In the same manner, cases ③ and ④ are almost identical so that difference cannot be seen in the figure; therefore, only one result is shown as red dotted line. There are slight differences between two lines, but difference can be negligible in the engineering practice. It shows that β=0.005 is sufficiently small.

Comparison between cases ② and ⑤ is compared in Fig. 13. There are non-negligible difference between them. This indicates that evaluation of velocity dependent characteristics is important.

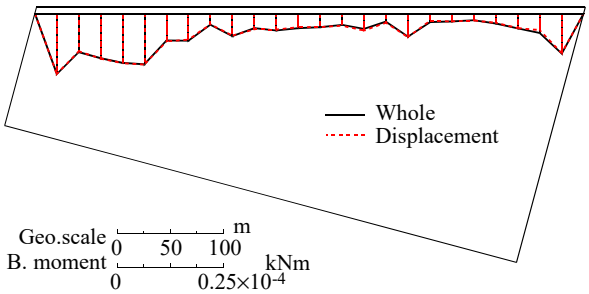

Fig. 12 – Maximum bending moment

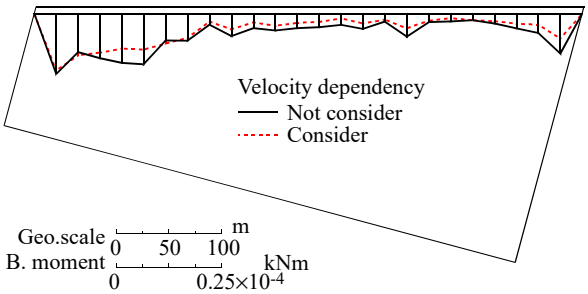

Fig. 13 – Maximum bending moment

5. Underground lineal structure with T shape connection

There are two types of damage of the underground lineal structure. One occurs slip out of junction or compressive collapse, which occurs in lineal portion, and the other is damage at a joint such as cross or T-shape connection. Same as the previous chapter, these damage does not occur under vertically propagating earthquake motion, therefore, analysis of the structure becomes multiple support excitation analysis.

An underground water supply pipeline with T shape connection schematically shown in Fig. 14(a) is analyzed. The pipeline is same with the previous one. The earthquake motion is assumed to incident 45 degrees from vertical and longitudinal direction of the pipeline as shown in Fig. 14(b).

Mechanical properties of the interaction spring in the previous chapter is modeled based on Shimamura et al. [11]. The pipeline used in this test is a corrugated pipeline, a steel pipeline with polyethylene coating, which is different from the water supply pipeline. One of the author conducted pull out test of polyethylene water supply pipelines in the sand ground in order to obtain velocity dependent characteristics between soil and pipeline [12]. In is found that velocity dependent property is hardly observed,

and that friction coefficient is about 0.5. Ultimate strength increases 1.2 to 1.4 times larger under fast loading. Kobayashi et al. [13] conducted cyclic loading test on polyethylene coated steel pipelines and showed that hysteretic characteristics can be modeled by a bi-linear model whose ultimate stress is 5 to 9kN/m^2. These two researches shows harmonic conclusions. Therefore, coefficient of subgrade reaction is set 6 MN/m^3, and ultimate shear stress is set 5 kN/m^2. No velocity proportional characteristics is considered.

Since applicability of the multi exciting formulation is proved in the previous chapters, the whole analysis is not conducted here. Same as previous example, shear wave velocity of the ground is 150 m/s; apparent wave velocity is 106 m/s. One sinusoidal wave with maximum amplitude 0.5 m/s and with frequencies 5, 1, and 0.5 Hz is applied. Since whole analysis is not conducted, reflected wave at the ground surface is not considered.

Maximum bending moment of the pipeline is shown in Fig. 15. Fig. 15(a) is the result when interaction spring is elastic. It is zero at the end because boundary condition at the end of the pipeline is set rotation free. It is nearly constant along linear part, and changes at the connection. It is the largest when frequency of the sinusoidal wave, *f*, is 5 Hz, possibly because curvature of the ground is largest as it is proportional with frequency.

Fig. 15(b) compares maximum bending moment under nonlinear behavior when *f*=1 Hz. Here, nonlinear 1 in the figure is the result when static nonlinear stress-displacement relationships is used, and nonlinear 2 uses ultimate stress 1.4 times larger than the one of static case. Maximum bending moment under nonlinear behavior is much smaller than that under the elastic behavior.

Fig. 16 shows stress-strain relationships in the nonlinear 1 case (ultimate stress = 5 kN/m^2). Amplitude of the velocity is set same in this case study, which means displacement amplitude is larger as input frequency becomes smaller. Therefore, displacement of the interaction spring is largest when *f*=0.2 Hz.

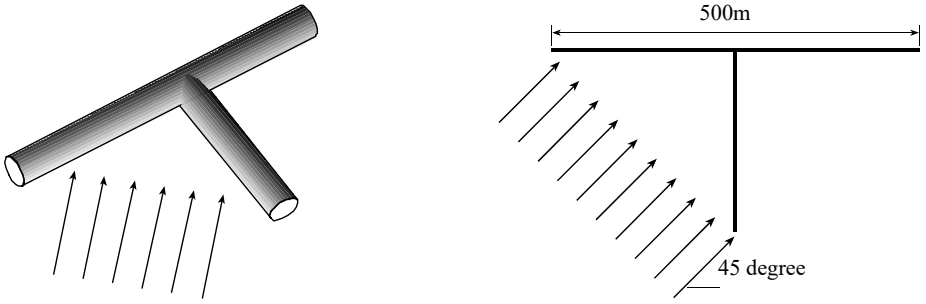

(a) Image of analyzed model (b) Plan of model

Fig. 14 – Analyzed model

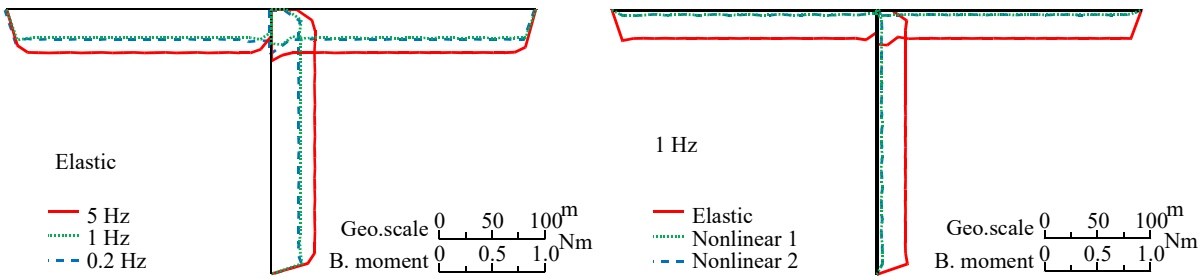

(a) Elastic interaction spring (b) Nonlinear vs. elastic

Fig. 15 – Maximum bending moment

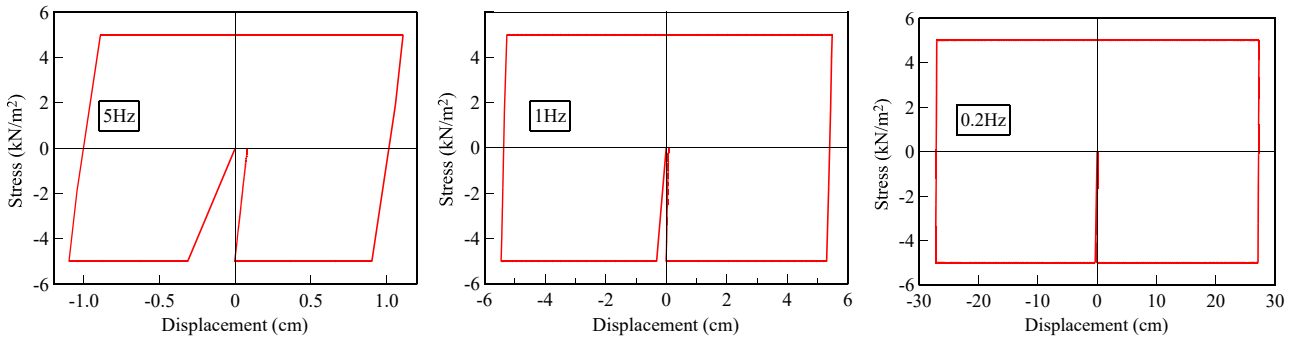

(a) 5 Hz (b) 1 Hz (c) 0.2 Hz

Fig. 16 – Stress-displacement relationships of interaction spring

In chapters 5 and this chapter, it is shown that both inertial force and velocity input is not necessary; analysis can be done by specifying displacement. Displacement can be applied both by statically and by dynamically. Both methods are shown to give same result in chapter 4.

If displacement is applied dynamically, it may be interested how velocity and acceleration are. Since it is not calculated automatically in the computer program, it is to be calculated separately. Fig. 17(a) shows displacement input when frequency of the wave is 1 Hz. Ideally, only 1 sinusoidal wave is intended to apply, which is shown as black solid line, but in the computer program, nontrivial zero is to be added as shown in red solid line with circle, where circle is the time when displacement is given.

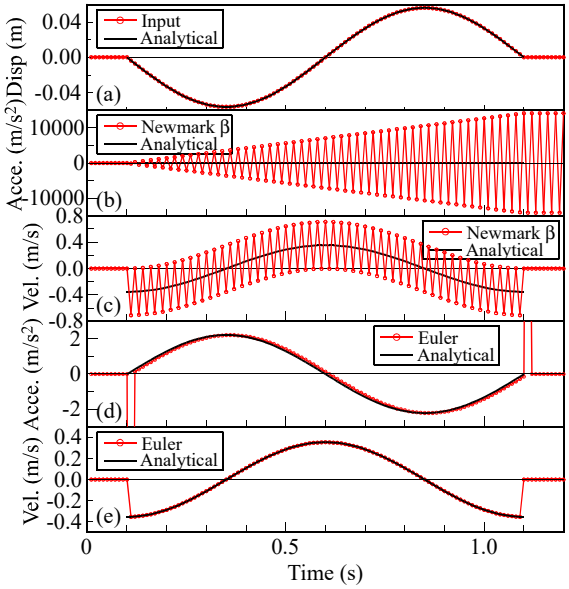

Fig. 17 – Comparison of integration schemes

Incremental equation of the Newmark's β method, which is used in the preceding analysis, is expressed as

$$\begin{aligned} d\dot{u} &= dt\ddot{u} + \gamma dt d\ddot{u} \\ du &= dt\dot{u} + 0.5dt^2\ddot{u} + \beta dt^2 d\ddot{u} \end{aligned} \tag{15}$$

Velocity increment is calculated from Eq. (15). Acceleration increment is obtained from displacement increment as

$$d\ddot{u} = \frac{du - dt\dot{u} - 0.5dt^2\ddot{u}}{\beta dt^2} \tag{16}$$

Then both velocity and acceleration increments are calculated from specified displacement incerement. Result of calculation is shown in Fig. 17(b)(c). Velocity response vibrates around the analytical response and acceleration increase monotonically. It is noted that value of absessa is very large; analycal line looks horizontal line. This indicates that Newmark's β method is not relevant in this kind of calculation.

They are also calculated by the Euler backward difference method from the displacement increment as

$$d\dot{u} = du / dt, \quad d\ddot{u} = d\dot{u} / dt \tag{17}$$

Result of calculation is shown in Fig. 17(d)(e). Both velocity and acceleration responses are well simulated except that acceleration at the beginning and at the end of the sinusoidal wave. Acceleration response shows pulse peak (35.3 m/s^2). The reason of this pulse is clear; as shown in Fig. 17(a), slope of displacement is not continuous at these points. This means that input displacement time history is better to be natural one, i.e., that does not have discontinous slope.

6. Concluding remarks

Applicability of the multiple support excitation formulation for underground structures is examined. Obtained conclusions and notes to use the formulation are as follows.

Multiple support excitation analysis gives results same with the whole analysis in which structures and grounds are solved simultaneously. The conventional computer program need to add function to consider velocity and displacement input. However, it is shown that inertia force hardly affects the response, and can be negligible. Therefor if there is no velocity dependent characteristics in the interaction spring, only displacement is required as input.

Velocity is not negligible in the first case study in chapter 3. Rayleigh damping (stiffness proportional damping) is used with coefficient β=0.005, which is not an extraordinary value but frequently used value. On the other hand, in the second case study in chapter 4, velocity dependent property does not affect the seismic response when β=0.0005, and velocity dependent property of the interaction spring is shown to affect the seismic response. It is noted that Rayleigh damping is the most frequently used damping in the seismic response analysis partly because it helps stability of numerical integration. It is usually evaluated from global mass and stiffness matrix. Therefore, special care is required in order to consider velocity dependent property relevantly because velocity dependent damping is automatically considered in the interaction spring.

In the third case study in chapter 5, ultimate strength is affective in the seismic response.

Considering these findings, mechanical property of the interaction spring is very important factor. Number of research is not many, and conclusions are different to each other. A research shows velocity dependent and another is not. A research shows ultimate strength and another is not. It may depend on materials. Actually, as shown in Fig. 11, mechanical properties are different between different sand. Therefore, research on this field in encouraged.

Acknowledgement

Research in chapter 3 is done as a part of works in committee on behavior and design of pile in liquefied ground. Research in chapters 4 and 5 was supported by JSPS KAKENHI Grant Number JP26289144. The authors gratefully acknowledged.

References

[1] Clough, R.W, Penzien, J: (1975) *Dynamics of structures*, McGraw-Hill Kogakusha, Tokyo

[2] Penzien, J., Scheffey, C F, Parmelee, A (1964): Seismic analysis of bridges on long piles, *Journal of the Engineering Mechanics Division (EM), Proc. ASCE,* **90**(EM3), 223-254

[3] Takagi, M, Kusakabe, K (1998): Dynamic analysis considering structure, foundation, and ground as one, *Proc., 5th symposium on dynamic interaction of structure and ground*, 87-96 (in Japanese)

[4] Proc., Symposium on Behavior and Design of Pile in Liquefied Ground, Japanese Geotechnical Society, 2004 (in Japanese)

[5] Tanaka, T., Yoshida, N., Kameoka, Y., Hasegawa, Y. (1983): Multiple support excitation analysis of underground structures, *Proc., 38th Annual Conf. of the Japan Society of Civil Engineering*, I, 49-50 (in Japanese)

[6] Horikoshi, K., Tateishi, A., Ohtsu, H. (2000): Detailed investigation of piles damaged by Hyogoken Nambu earthquake, *Proc. of 12th World Conference on Earthquake Engineering*, Auckland, Paper No. 2477

[7] Yoshida, N., Tsujino, S., Ishihara, K. (1990): Stress-strain model for nonlinear analysis of horizontally layered deposit, *Summaries of the Technical Papers of Annual Meeting of AIJ*, Chugoku, (B), 1639-1640 (in Japanese)

[8] Japan Road Association (1996): *Specifications for Highway Bridges*, Part V, Seismic design (in Japanese)

[9] Kishida, H. and Nakai, S. (1979): Analysis of a lateral loaded pile with non-linear subgrade reaction, *Transactions of the Architectural Institute of Japan*, (**281**), 41-55 (in Japanese)

[10] Japan Water Supply Association （JWWA) (2009): Earthquake-proof Method Criteria for Waterworks (in Japanese)

[11] Shimamura, K., Takenouchi, H., Miki, C. and Fukazawa, K. (1999): A real scale experimental study on dynamic soil spring characteristics in axial direction for buried pipeline, *Proc. JSCE*, **612/I-46**, 55-66 (in Japanese)

[12] Kuwata, Y., Inase, T., Sawada, S. (2017): Modeling of axial soil spring based on pipe pulling test considering velocity dependency, *Proc. 37th JSCE Earthquake Engineering Symposium-2017*, Paper No. B24-1136 (in Japanese)

[13] Kobayashi, M., Ando, H., and Oguchi, N. (1998): Effects of velocity and cyclic displacement of subsoil on its axial restraint force acting on polyethylene coated steel pipes during earthquakes, *Proc. of JSCE*, **591/I-43**, 299-312 (in Japanese)

